JCTC Journal of Chemical Theory and Computation

Letter

pubs.acs.org/JCTC

Improved Treatment of Surrounding Effects: UV/vis Absorption Properties of a Solvated Ru(II) Complex

Agisilaos Chantzis, Thibaut Very, Antonio Monari,* and Xavier Assfeld

Equipe de Chimie et Biochimie Théoriques, SRSMC UMR 7565, Université de Lorraine—Nancy and CNRS, Boulevard des Aiguilletes BP 70239, 54506 Vandoeuvre-lès-Nancy, France

Supporting Information

ABSTRACT: The UV/vis and circular-dichroism spectra of a bis-bipyridinyl ruthenium complex are computed at the density functional theory level and the time dependent density functional level of theory. The effects of the solvent, here water, have been taken into account, by polarizable continuum methods and by a hybrid quantum-mechanics/molecular-mechanics approach combined with molecular dynamics. The effects of the solvent have been decomposed in geometric, electrostatic, and polarization of the environment. The principal transitions have been analyzed by means of natural transition orbitals.

Ruthenium organometallic complexes are nowadays among the most important classes of organometallic compounds, and their rather peculiar photochemical and photophysical properties[1,2] are exploited in different fields and applications. In particular, ruthenium complexes have been the basic components of dye-sensitized-solar cells from the very beginning of such technology and are still today among the most efficient dyes.[3−6] In a totally different field, ruthenium polypyridyl complexes have been recognized as very efficient DNA probes since they are capable of a quite important interaction with such a fundamental macromolecule. Moreover, the photophysical properties of the complex may change radically upon interaction with DNA; in some cases, the fluorescence, present in aqueous media, is indeed quenched by DNA interaction, while in other cases the nonemitting solvated complex shows an intense fluorescence upon the addition of DNA.[7−12] Such a phenomenon has been identified as a sort of light-switching effect and has potentially extremely important applications in DNA recognition, but also in sensitive diagnostics, chemotherapeutics, and phototherapy. Indeed, ruthenium complexes have shown a potential use as an antitumoral drug, being able to cause irreversible DNA damage, most probably because of intercalation and of a subsequent excited state mediated charge transfer process.[13] It is evident that, because of the extremely complex nature of the process involved, a good understanding of the photophysical processes involved in such phenomena is of seminal importance to improve the recognition and potential therapeutic properties of such systems. This is also the reason why a large number of experimental studies, mainly spectroscopic and theoretical computations on such systems have appeared.[14−16] Actually, because of the light-switching properties, the correct modelization of the environmental effects is also extremely important to correctly reproduce the properties of the known complexes, to formalize the interaction mechanism, and to correctly preview and model the behavior of different molecules. It is to be emphasized that taking into account correctly the environment effects in such complex media is quite a difficult task for computational and quantum chemistry; for instance, some studies on the interaction of two DNA base pairs and bipyridyl Ru complexes have been reported.[17] Among DNA light switching compounds, the ruthenium bis-bipyridinyl (bipy) dipyridophenazine (dppz) dication (general formula Ru-[bipy$_2$dppz]$^{2+}$), see Figure 1, has been one of the first complexes to be considered and one of the most extensively studied, since it shows a very intense fluorescence only when complexed by DNA.[18] Moreover the presence of the planar dppz ligand is able to favor the DNA intercalation. The computational study of the intercalated adduct, and of its absorption properties, will be reported elsewhere.

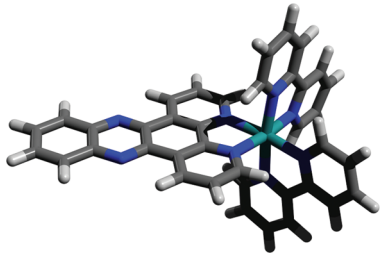

Figure 1. The Ru[bipy$_2$dppz]$^{2+}$ complex.

In the present contribution, we will focus on the absorption properties in water, on the role played by the solvent and on the different treatments of the environment. In particular, we will compare two different strategies: the first one is based on the use of the polarizable continuum medium (PCM)[19] technique to implicitly take into account the electrostatic effects of the environment; the second one will be based on the combined use of classical molecular dynamics (MD) and mixed quantum-mechanics molecular-mechanics (QM/MM) techniques to take into account the medium as well as its dynamic behavior in a statistical meaningful way.[20] Indeed, the use of mixed QM/MM methods and PCM to recover an absorption spectrum and in general excited state properties in complex

Received: February 14, 2012
Published: April 12, 2012

media is nowadays a very active field of research.[21−23] The two approaches have been compared, and the different contributions influencing the general behavior of the absorption spectra will be presented and analyzed. The validation of the MD plus QM/MM based method for a molecular system (Ru octahedral complex) for which good force field parameters are not easily available is extremely important before attempting the dynamical description of more complex systems (i.e., the interaction with DNA); strategies to overcome such limitations at a moderate computational cost will be presented here. Moreover, the importance of the polarization effect of the environment at the QM/MM level will be emphasized, and its influence will be taken into account by using the so-called electronic response of the surroundings (ERS)[17,25−29] technique, that combines good accuracy with a moderate cost and the possibility to use classical nonpolarizable force fields to treat the MM systems. The present letter is organized as follows: after a description of the strategies and methods used, the Computational Details will be presented, allowing us to present and analyze our results and finally draw our conclusions and future perspectives.

COMPUTATIONAL STRATEGIES

As already stated, two main approaches are usually considered when trying to compute absorption spectra of solvated molecules:[20] either to consider implicitly the effects of the environment introducing a continuum medium characterized by its dielectric constant ε or to explicitly include the solvent molecules into the system. Of course, because of the system size (usually many thousands of solvent molecules for each solute), one has to rely on a hybrid QM/MM description of the system where the solute is treated at the quantum level of theory and the solvent is described using a molecular mechanics force field, even if recently some full QM treatments using semiempirical methods have been proposed.[30] Of course, a solute molecule surrounded by solvent is by nature a quite dynamic system: many configurations accounting for different distributions of the solvent are possible with almost equal probability. Different solvent distributions will also induce a slight geometric deformation on the solute molecule. This implies that one cannot treat the system with a static approach only computing the absorption spectrum as vertical (Franck−Condon) transitions arising from the equilibrium geometry. The only way to get a meaningful statistical description of the system is to perform sufficiently long dynamics, allowing to get a trajectory from which random snapshots are extracted in order to compute excited states and transitions. The final spectrum will then be the average of all of the single points spectra. When dealing with $Ru[bipy_2dppz]^{2+}$ of course the use of classical molecular mechanics would be preferable since its limited computational cost would allow one to run longer trajectories and therefore to better explore the configuration space. The main problem arising is the lack of force fields able to correctly reproduce the octahedral geometrical arrangement of the ruthenium complex; indeed, some preliminary MM optimization produced a totally meaningless and distorted equilibrium geometry. To overcome such a problem without having to rely on a quite expensive QM/MM Born−Oppenheimer dynamics technique, we propose the following procedure: first a molecular mechanics trajectory is run freezing the coordinates of the whole Ru complex, allowing us to take into account the different solvent distributions. From the trajectory, some random snapshots are extracted, and a QM/MM optimization of the $Ru[bipy_2dppz]^{2+}$ complex is performed freezing the coordinates of the MM part (i.e., of the solvent molecules). This step allows one to recover, at least partially, the geometrical relaxation of the complex to the solvent molecules' movement and therefore to take into account its flexibility. Finally, excited states are computed from each "optimized" snapshot, in the framework of the Franck−Condon principle, and the final spectrum is obtained as the average. If the previous emphasized strategy allows one to recover the geometrical relaxation effects, a pure QM/MM treatment done with a classical nonpolarizable force field is still lacking an important contribution to the excited state description. Indeed, if the Franck−Condon principle dictates that the chromophore and the solvent molecules do not rearrange upon the transition, i.e., all transitions are vertical, this is not true for the electronic cloud of the solvent molecules that can polarize and adapt to the excited state. A possibility to recover such a physical phenomenon is to embed the MM part into a continuum characterized by a dielectric constant extrapolated at infinite frequency (ε_∞), also called a dynamic, fast, or electronic dielectric constant. This technique,[17,25−29] called ERS, was proven efficient in recovering such an effect, whose magnitude has been shown to be comparable to the pure electrostatic effects of the MM point charges. Since the value of this dielectric constant is practically constant for insulator species varying in a range comprised from 1.5 and 2.0 au, a common value of 1.776 has been chosen to treat organic and water solvent and environments.

COMPUTATIONAL DETAILS

For all of the QM calculations we have considered the DFT[31] and TD-DFT[31,32] approach; pure QM calculations have been performed by the Gaussian 09 code.[33] QM/MM calculations have been performed by using a local modified version of Gaussian 09[34,35] code interfaced with Tinker code[36] for the MM part; Tinker has also been used to perform the MM dynamics. The LANL2DZ basis set,[37] with pseudopotential on the Ru atom, and the B3LYP[38,39] exchange-correlation functional have been used throughout, and 70 excited states have been computed with TD-DFT. In the case of PCM calculations, the standard parameters for water dielectric constant and cavity as provided in Gaussian 09 have been used; in the case of the ERS technique the QM region has been placed in a molecular cavity based on the van der Waals radii. One has to note that the QM part is now surrounded by the MM part and by the continuum, the MM part being immersed in the continuum and not interacting with it.

Some benchmarks done on the isolated system showed that the use of a larger basis set (triple-ζ) did not change significantly the spectrum. On the other hand, the use of the long-range corrected CAM-B3LYP[40] functional produced a degradation of the spectrum, even in the charge transfer region, with transition being generally blue-shifted by almost 100 nm compared to experimental values (see Supporting Informations). This rather surprising behavior can be ascribed to the fact that even charge-transfer transitions are taking place between relatively spatially close regions. Indeed, when applying the analysis based on the overlap between occupied and virtual orbitals, as proposed by Peach et al.,[41] we obtain, for all the most intense transitions, a value of the λ parameter comprised between 0.75 and 0.89, i.e., well above the proposed limit of applicability for B3LYP ($\lambda > 0.3$). Preliminary molecular dynamics has been realized solvating Ru-

$[bipy_2dppz]^{2+}$ with 4182 water molecules on a cubic box of 50 × 50 × 50 Å size (see Figure 2). Since the ruthenium complex

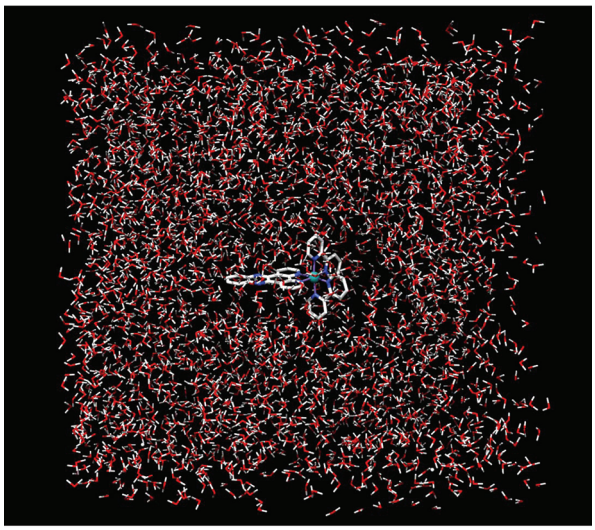

Figure 2. One snapshot of the simulation, water in wires representation and $Ru[bipy_2dppz]^{2+}$ in sticks (note that hydrogens belonging to the complex have not been represented for clarity reasons).

has a +2 charge, two chlorine anions have been added to obtain a neutral box; periodic boundary conditions have been used throughout. Water molecules have been treated using the TIP3P model.[42] The dynamics were performed under constant volume and temperature (NVT ensemble) with the temperature being set at 310 K and with a 2.0 fs time-step for a total of 200 ps. As can be seen from Figure 3, the system can be

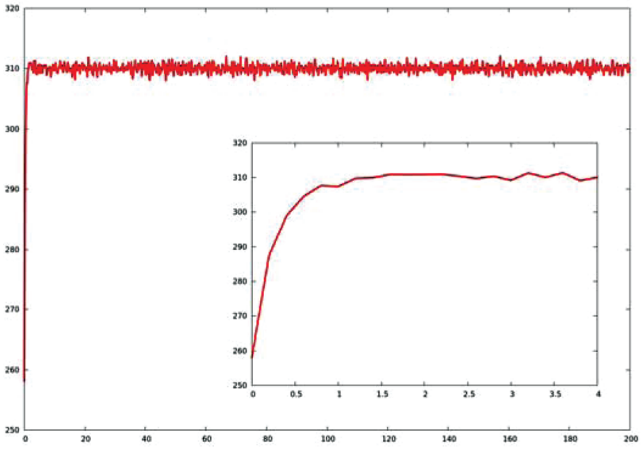

Figure 3. The temperature T evolution (time in ps, T in K) over the molecular dynamics. In the box, a zoom of the first steps.

considered as stabilized after about 3 ps. Snapshots have been extracted all over the stabilized region, i.e., from 3 to 200 ps, the minimal distance between different snapshots being about 500 ps. To ensure the statistical significance of our sampling, we checked the value of the time autocorrelation function for the velocities (see the Figure in the Supporting Information) that appears converged to zero just after about 100 fs, so that validating our choice.

RESULTS AND DISCUSSIONS

As a first step, we have checked the statistical stability of the averaged spectrum over different samples. In Figure 4a, we report the absorption spectrum obtained with a set of 10, 20, and 30 snapshots, respectively. Note that in this case QM/MM spectra have been obtained by considering electrostatic and polarization (ERS) contributions. As one can see, the three sets are almost indistinguishable, implying that the smaller 10 snapshots set is already sufficient to represent the behavior of the system. On this basis, one can safely compare the behavior of the QM/MM + ERS spectra with the one obtained with the implicit treatment of the solvent (linear response PCM), and with experimental results,[43] as is done in Figure 4b. Note also that the spectrum has been constructed by convoluting each vertical transition with a Gaussian function of fixed half length width of 0.2 eV. The value of the maximum absorption wavelengths for the different bands are reported in the Supporting Information.

As one can see, both PCM and QM/MM+ERS spectra are able to reproduce the most important features of the experimental spectrum. In particular, the charge-transfer band at about 450 nm and the most intense band in the near UV centered at around 290 nm. Between the two, on the experimental spectrum, one can see a large and not well resolved band that is less well reproduced by both approaches. Indeed, looking closer at such a region, one can see that some transitions, but with small intensities, are previewed. One can also see that, even if quite similar, the QM/MM + ERS approach shows general broader bands than the PCM one. Also, notice that in the computed spectra some very weak MLCT transitions are evidenced between 500 and 600 nm. Since the experimental spectrum shows a large band centered at 450 nm, and because at these wavelengths a weak error in the energy of the excited states could induce a significant shift, we think that the latter weak transitions are indeed embedded in the large experimental band.

If both PCM and QM/MM + ERS approaches appear able to reproduce the convoluted behavior of the spectrum, some differences appear when one looks at the vertical transitions only. In Figure 5, we report the vertical transitions for the PCM and for the PCM + ERS methodology. In the case of QM/MM + ERS, both wavelengths and oscillator strengths have been obtained as the average over 30 snapshots. First of all, note that QM/MM + ERS previews many transitions, although of weak intensity, in the region around 350−400 nm, i.e., the region characterized by the broad non-well-resolved band in the experimental spectrum, suggesting that indeed this region could be reproduced even if intensities are not very well described. The most striking difference is indeed seen on the 290 nm band; in fact, if both bands appear similar when looking at the convoluted spectra, the PCM one is determined by two strongly dominating transitions, while in the case of QM/MM + ERS the band is constituted of a large number of transitions with relatively weak intensity whose collective effect gives rise to the high intense absorption. In Figure 6, we report the spectrum computed as the average over 30 snapshots taking into account electrostatic and polarization effects (QM/MM + ERS) and only the electrostatic (QM/MM) and discarding both of them, i.e., setting to zero the MM point charges (geometric in the figure).

The spectra presented up to now included, as already mentioned, both electrostatic and polarization (ERS) effects. It

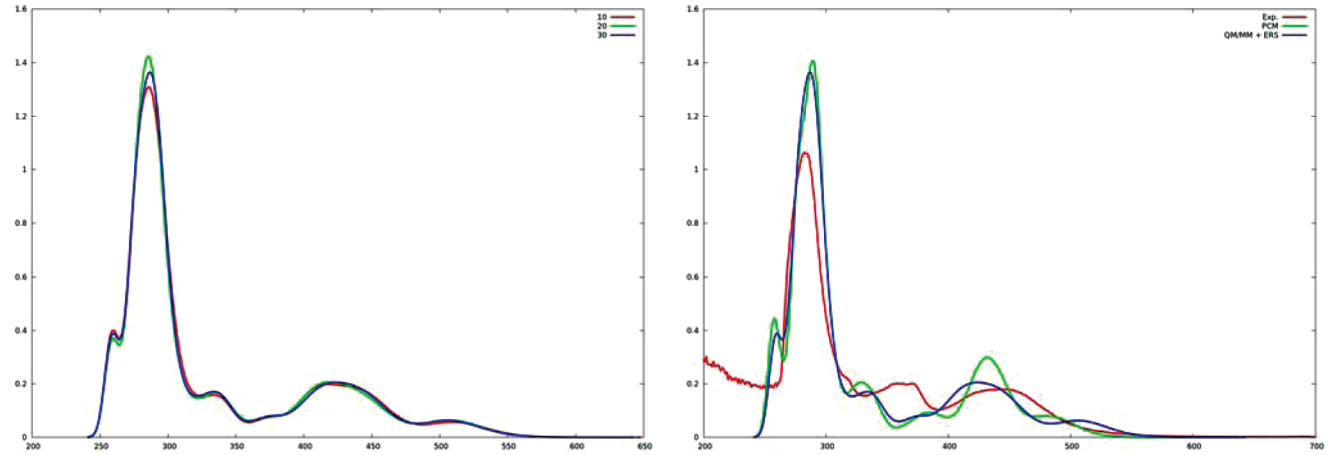

Figure 4. (a) The QM/MM + ERS UV/vis spectrum averaged over a different number of snapshots. (b) The comparison between the QM/MM + ERS spectrum (average over 30 snapshots), PCM, and experimental results. Wavelengths in nm, intensities in arbitrary units.

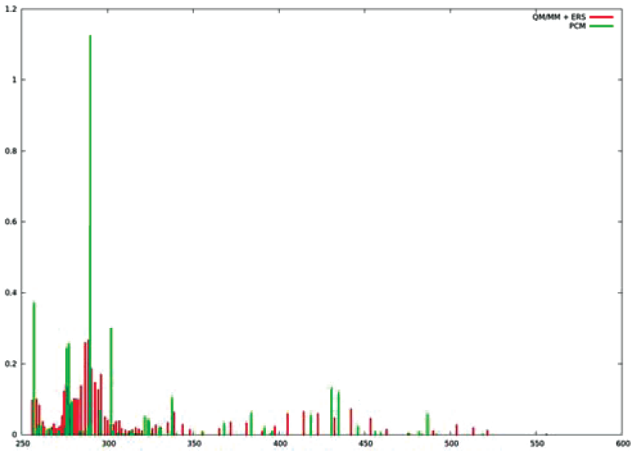

Figure 5. The vertical transition for QM/MM + ERS and PCM spectra. Wavelengths in nm. Intensities in arbitrary units.

is interesting to analyze them ignoring one or both of the effects to monitor their relative influence. As one can see, the inclusion of the ERS contribution appears important to recovering a correct behavior and shape of the spectrum. Discarding them will produce a much broader and less

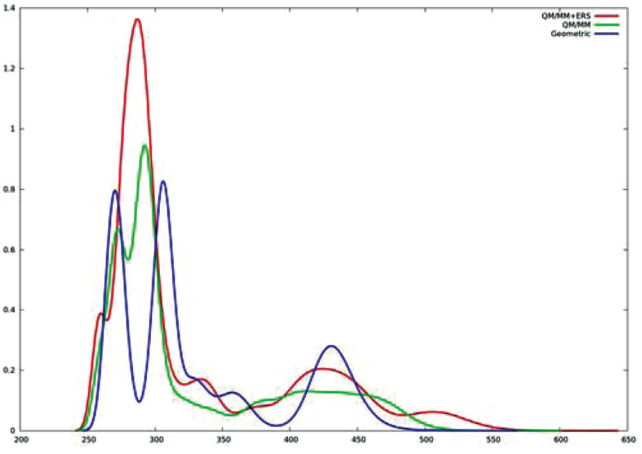

Figure 6. Spectra computed with and without electrostatic and polarization effects.

structured charge transfer band, while the intense 290 nm band starts to split into two contributions, at the same time losing practically all contributions in the region between the two. Of course, discarding also electrostatic effects leads to an even more dramatic deviation with the most intense band now being split into two well-defined bands. These aspects show that to recover a correct behavior of UV/vis spectra it is important to take care of all three contributions, even for cationic species like the present one, for which pure electrostatic effects could have been thought to prevail largely.

In order to better evaluate the stability of the linear response PCM (LR-PCM) approach, we decided to consider the nonequilibrium state specific PCM (SS-PCM) solutions as proposed by Improta et al.[44,45] in which the energy of the excited state in solution is computed by making the solvent reaction field self-consistent with the solute electrostatic potential in the excited state of interest. The latter strategy, although extremely sound, is much more computationally costly and, in opposition to the linear response formalism, necessitates a separate treatment for each excited state. We chose to consider a low energy MLCT state (the 10th excited state, 432 nm) and an intraligand charge transfer excited state (the 21st excited state, 337 nm). For the MLCT case, the SS-PCM gives an excitation energy of 2.852 eV, while the LR-PCM gives an excitation at 2.867 eV. In the case of the intraligand transition, the two approaches give an excitation of 3.617 and 3.677 eV, respectively. We should underline that the difference between LR- and SS-PCM depends on the ratio between the transition dipole and the variation of dipole moment associated with a given transition.[44] It will, therefore, be much more pronounced for weak transitions and dark states; for instance, in our case the weak intraligand transition corresponding to the 22nd excited state shows a difference of 0.2 eV between the two approaches. In any case, our findings confirm, as already stated for instance by Improta et al.,[44] that LR-PCM is able to recover the main characteristic of the excitation spectrum at a much more limited computational cost.

The same general behavior, illustrated for the absorption spectrum, is also confirmed by the circular-dichroism (CD) spectrum presented in Figure 7 for the Δ isomer. (Rotatory strengths have been calculated with the "velocity" approximation). Note that in this case the differences with PCM are quite amplified, in particular in the region between 400 and 450 nm. Probably, since this part of the spectrum is dominated by

dx.doi.org/10.1021/ct300129c | J. Chem. Theory Comput. 2012, 8, 1536−1541

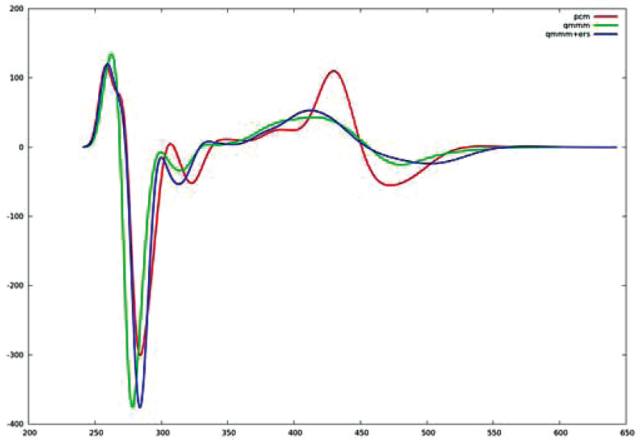

Figure 7. Computed CD spectrum. Wavelenghts in nm, intensities in arbitrary units.

metal to ligand charge transfer, this behavior is due to a different sensitivity to the ligand geometry deformation between the two approaches. Indeed, one can see from Figure 8a that our approach allows one to take into account quite an

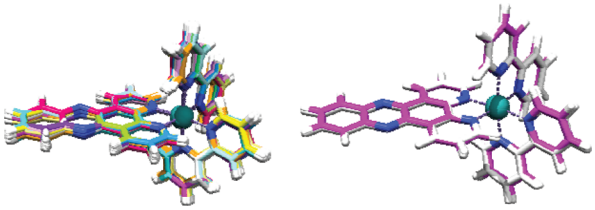

Figure 8. (a) The superposition of the different snapshots geometry, after QM/MM optimization, and (b) superposition of PCM optimized geometry with the average geometry of the previous snapshots.

important deformation of the ligand geometries between different snapshots, while on the other hand the average geometry over the different snapshots appears quite well superposable, even if not identical to the one obtained at PCM level (Figure 8b).

The nature of the excited states giving rise to the UV/vis spectrum is analyzed making use of the NTO formalism.[29,31,46] Results for transitions giving rise to the three most intense spectroscopic bands are reported in Figure 9. As expected, one can see that in the high wavelength region, the spectrum is constituted by metal to ligand charge transfer transitions. In particular, the transition represented here (451 nm) shows a dominant participation of the dppz moiety in the virtual NTO. On the other hand, the large, less intense band comprised between 400 and 330 nm is more complicated and shows the presence of both mainly metal to ligand charge transfer (407 nm) and mainly intraligand transitions (336 nm). The last intense band is of course dominated by intraligand transitions. However, as shown in the 279 nm transition NTOs, care should be taken in analyzing such transitions; indeed, the transition is not a pure one but rather shows a less important, but not negligible, contribution from a metal to ligand charge transfer that has to be considered together with the bipy intraligand contributions. Such a mixed character of transition even at short wavelengths can have important consequences over the rather complicated photophysical properties exhibited by this kind of complex.

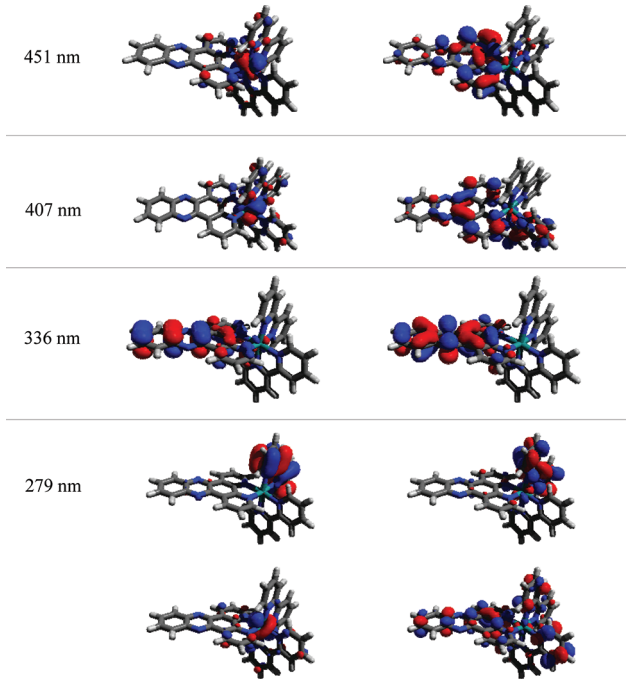

Figure 9. NTOs isodensity (0.03 threshold) surface for some selected transitions.

CONCLUSIONS

We have used a combination of molecular dynamics and QM/MM hybrid calculations to compute the absorption spectra in water of an important ruthenium organometallic complex that is used as a DNA intercalator. To overcome the limitations due to an insufficiently well parametrized force field, we have performed the MD keeping the complex geometry fixed and relaxing the latter at the QM/MM level on selected snapshots. The averaged spectrum has been compared to the PCM one and to experimental results, and one can see that the proposed strategy is able to recover the most important properties of the solute. In any case, in order to obtain correct results, one should take into account the polarization effects of the environment, since the electrostatic effects alone are definitively not sufficient to describe all of the aspects of the spectrum. Interestingly enough, even if the PCM and QM/MM spectra have a similar general shape, one can see that the intensity of the transitions is distributed differently in the two cases. The excited states, giving rise to the most intense transitions, have been analyzed, and the latter showed a complex mixed nature, with the presence of metal to ligand charge transfer character up to quite short wavelengths. Our results provide an important understanding of the behavior of this class of complexes in aqueous media and also constitute a validation of a strategy that will be used to determine absorption and emission properties in much more complex environments and in particular upon DNA intercalation.

ASSOCIATED CONTENT

Supporting Information

The B3LYP and CAM-B3LYP computed spectra are provided superposed with the experimental one. The figure illustrating the variation of velocity autocorrelation function with time is shown. A table reporting the absorption maxima for the UV/vis spectrum computed with the different strategies is presented.

dx.doi.org/10.1021/ct300129c | J. Chem. Theory Comput. 2012, 8, 1536−1541

This material is available free of charge via the Internet at http://pubs.acs.org.

AUTHOR INFORMATION

Corresponding Author

*E-mail: antonio.monari@univ-lorraine.fr.

Notes

The authors declare no competing financial interest.

ACKNOWLEDGMENTS

Support from Université de Lorraine and CNRS is gratefully acknowledge, also for the funding of the "Chaire d'excellence" (A.M.). We also acknowledge support from the ANR project ANR-09-BLAN-0191-01 "PhotoBioMet". We thank Michel Pfeffer and Stéphane Despax for having provided us the experimental UV/vis spectrum

REFERENCES

(1) Lebon, E.; Bastin, S.; Sutra, P.; Vendier, L.; Piau, R. E.; Dixon, I. M.; Boggio-Pasqua, M.; Alary, F.; Heully, J.-L.; Igau, A.; Juris, A. *Chem. Commun.* **2012**, *48*, 741.

(2) Guillon, T.; Boggio-Pasqua, M.; Alary, F.; Heully, J.-L.; Lebon, E.; Sutra, P.; Igau, A. *Inorg. Chem.* **2010**, *49*, 8862.

(3) Monari, A.; Assfeld, X.; Beley, M.; Gros, P. C. *J. Phys. Chem. A* **2011**, *115*, 3596.

(4) Nazeeruddin, M. K.; De Angelis, F.; Fantacci, S.; Selloni, A.; Viscardi, G.; Liska, P.; Ito, S.; Takeru, B.; Grätzel, M. *J. Am. Chem. Soc.* **2005**, *127*, 16835.

(5) Grätzel, M. *Inorg. Chem.* **2005**, *44*, 6841.

(6) Hagfeldt, A.; Boschloo, G.; Sun, L.; Kloo, L.; Pettersson, H. *Chem. Rev.* **2010**, *110*, 6595.

(7) Olson, E. J. C.; Hu, D.; Hörmann, A.; Jonkman, A. M.; Arkin, M. R.; Stemp, E. D. A.; Barton, J. K.; Barbara, P. F. *J. Am. Chem. Soc.* **1997**, *119*, 11458.

(8) Labat, F.; Ciofini, I.; Hratchian, H. P.; Frisch, M.; Raghavachari, K.; Adamo, C. *J. Am. Chem. Soc.* **2009**, *131*, 14290.

(9) Labat, F.; Ciofini, I.; Hratchian, H. P.; Frisch, M.; Raghavachari, K.; Adamo, C *J. Chem. Phys. C* **2011**, *115*, 4297.

(10) Brennaman, M. K.; Meyer, T. J.; Papanikolas, J. M. *J. Phys. Chem. A* **2004**, *108*, 9938.

(11) Brenaman, M. K.; Alstrum-Acevedo, J. H.; Fleming, C. N.; Jang, P.; Meyer, T. J.; Papanikolas, J. M. *J. Am. Chem. Soc.* **2002**, *124*, 15094.

(12) Sun, Y.; Lutterman, D. A.; Turro, C. *Inorg. Chem.* **2008**, *47*, 6427.

(13) Delaney, S.; Pascaly, M.; Bhattacharya, P. K.; Han, K.; Barton, J. K. *Inorg. Chem.* **2002**, *41*, 1966.

(14) Sabatani, E.; Nikol, H. D.; Gray, H. B.; Anson, F. C. *J. Am. Chem. Soc.* **1996**, *118*, 1158.

(15) Pourtois, G.; Beljonne, D.; Moucheron, C.; Schumm, S.; Kirsch-De Mesmaeker, A.; Lazzaroni, R.; Brédas, J.-L. *J. Am. Chem. Soc.* **2004**, *126*, 683.

(16) Batista, E. R.; Martin, R. L. *J. Phys. Chem. A* **2005**, *109*, 3128.

(17) Ambrosek, D.; Loos, P.-F.; Assfeld, X.; Daniel, C. *J. Inorg. Biochem.* **2010**, *104*, 893.

(18) Friedman, A. E.; Chambron, J. C.; Sauvage, J. P.; Turro, N. J.; Barton, J. K. *J. Am. Chem. Soc.* **1990**, *112*, 4960.

(19) Tomasi, J.; Mennucci, B.; Cammi, R. *Chem. Rev.* **2005**, *105*, 2999.

(20) Mennucci, B. The simulation of UV-VIS Spectroscopy with Computational Methods. In *Computational Spectroscopy: Methods, Experiments, Applications*; Grunberg, J., Ed.; Wiley-VCH: Weinheim, Germany, 2010; p 151.

(21) Hoffman, M.; Wanko, M.; Strodel, P.; Köning, P. H.; Frauenheim, T.; Schulten, K.; Thiel, W.; Tajkhorschid, E.; Elstner, M. *J. Am. Chem. Soc.* **2006**, *128*, 10808.

(22) Curutchet, C.; Scholes, G. D.; Mennucci, B.; Cammi, R. *J. Phys. Chem. B* **2007**, *111*, 13253.

(23) Pedone, A.; Prampolini, G.; Monti, S.; Barone, V. *Phys. Chem. Chem. Phys.* **2011**, *13*, 16689.

(24) Jacquemin, D.; Mennucci, B.; Adamo, C. *Phys. Chem. Chem. Phys.* **2011**, *13*, 16987.

(25) Loos, P.-F.; Dumont, E.; Laurent, A. D.; Assfeld, X. *Chem. Phys. Lett.* **2009**, *475*, 120.

(26) Laurent, A. D.; Assfeld, X. *Interdiscip. Sci. Comput. Life Sci.* **2010**, *2*, 38.

(27) Jacquemin, D.; Perpète, E. A.; Laurent, A. D.; Assfeld, X.; Adamo, C. *Phys. Chem. Chem. Phys.* **2009**, *11*, 1258.

(28) Dumont, E.; Laurent, A. D.; Loos, P.-F.; Assfeld, X. *J. Chem. Theory Comput.* **2009**, *5*, 1700.

(29) Monari, A.; Very, T.; Rivail, J.-L.; Assfeld, X. *Comp. Theor. Chem.* **2011**, DOI: http://dx.doi.org/10.1016/j.comptc.2011.11.026.

(30) Ingrosso, F. F.; Monard, G.; Farag, M. H.; Bastida, M.; Ruiz-López, M. F. *J. Chem. Theory Comput.* **2011**, *7*, 1840.

(31) Dreuw, A.; Head-Gordon, M. *Chem. Rev.* **2005**, *105*, 4009.

(32) Runge, E.; Gross, E. K. U. *Phys. Rev. Lett.* **1984**, *52*, 997.

(33) Frisch, M. J.; Trucks, G. W.; Schlegel, H. B.; Scuseria, G. E.; Robb, M. A.; Cheeseman, J. R.; Scalmani, G.; Barone, V.; Mennucci, B.; Petersson, G. A.; Nakatsuji, H.; Caricato, M.; Li, X.; Hratchian, H. P.; Izmaylov, A. F.; Bloino, J.; Zheng, G.; Sonnenberg, J. L.; Hada, M.; Ehara, M.; Toyota, K.; Fukuda, R.; Hasegawa, J.; Ishida, M.; Nakajima, T.; Honda, Y.; Kitao, O.; Nakai, H.; Vreven, T.; Montgomery, J. A., Jr.; Peralta, J. E.; Ogliaro, F.; Bearpark, M.; Heyd, J. J.; Brothers, E.; Kudin, K. N.; Staroverov, V. N.; Kobayashi, R.; Normand, J.; Raghavachari, K.; Rendell, A.; Burant, J. C.; Iyengar, S. S.; Tomasi, J.; Cossi, M.; Rega, N.; Millam, N. J.; Klene, M.; Knox, J. E.; Cross, J. B.; Bakken, V.; Adamo, C.; Jaramillo, J.; Gomperts, R.; Stratmann, R. E.; Yazyev, O.; Austin, A. J.; Cammi, R.; Pomelli, C.; Ochterski, J. W.; Martin, R. L.; Morokuma, K.; Zakrzewski, V. G.; Voth, G. A.; Salvador, P.; Dannenberg, J. J.; Dapprich, S.; Daniels, A. D.; Farkas, Ö.; Foresman, J. B.; Ortiz, J. V.; Cioslowski, J.; Fox, D. J. *Gaussian 09*, Revision B.1; Gaussian, Inc.: Wallingford, CT, 2009.

(34) Ferré, N.; Assfeld, X.; Rivail, J.-L. *J. Comput. Chem.* **2002**, *23*, 610.

(35) Assfeld, X.; Rivail, J.-L. *Chem. Phys. Lett.* **1996**, *266*, 100.

(36) Tinker code package: http://dasher.wustl.edu/tinker/ (accessed April 8, 2012)

(37) Wadt, W. R.; Hay, P. J. *J. Chem. Phys.* **1985**, *82*, 284.

(38) Becke, A. D. *J. Chem. Phys.* **1993**, *98*, 1372.

(39) Lee, C.; Yang, W.; Parr, R. G. *Phys. Rev. B* **1993**, *37*, 785.

(40) Yanai, T.; Tew, D.; Handy, N. *Chem. Phys. Lett.* **2004**, *393*, 51.

(41) Peach, M. J. G.; Benfield, P.; Helgaker, T.; Tozer, D. J. *J. Chem. Phys.* **2008**, *128*, 044118.

(42) Jorgensen, W. L.; Chandrasekhar, J.; Madura, J. D.; Impey, R. W.; Klein, M. L. *J. Chem. Phys.* **1983**, *79*, 926.

(43) Michel Pfeffer and Sthéphane Despax, University of Strasbourg. Private communication.

(44) Improta, R; Barone, V.; Scalmani, G.; Frisch, M. J. *J. Chem. Phys.* **2006**, *125*, 054103.

(45) Improta, R; Scalmani, G.; Frisch, M. J.; Barone, V. *J. Chem. Phys.* **2007**, *127*, 074504.

(46) Martin, R. L. *J. Chem. Phys.* **2003**, *118*, 4775.